PROGRESS IN TWO-DIMENSION COLLECTIVE HAMILTONIAN FOR CHIRAL MODES*

X.H. Wu, S.Q. Zhang†

State Key Laboratory of Nuclear Physics and Technology, School of Physics
Peking University, Beijing 100871, China

(Received December 28, 2017)

The significant progresses of chirality in atomic nuclei from both experimental and theoretical sides are briefly reviewed. The recent progress of collective Hamiltonian for chiral modes is introduced. The results of collective Hamiltonian for an asymmetric particle–hole configuration $\pi g_{9/2}^{-1} \otimes \nu h_{11/2}$ coupled to a triaxial rotor are presented.

DOI:10.5506/APhysPolBSupp.11.199

1. Introduction

Since the pioneering work of Frauendorf and Meng in 1997 [1], nuclear chirality has attracted continuous and significant attention for two decades [2–5]. The spontaneous chiral symmetry breaking can happen in the intrinsic frame for a nucleus with triaxial deformed shape and high-j particle–hole configuration. In such a circumstance, the collective angular momentum of the triaxial core favors alignment with the intermediate (i) axis, and the angular momentum vectors of particle-like valence proton (neutron) and hole-like valence neutron (proton) align along the nuclear short (s) and long (l) axis, respectively. The three angular momenta are nearly perpendicular to each other and form two systems with opposite chirality, namely a left- and a right-handedness. A schematic picture of the left- and right-handed chiral systems is illustrated in Fig. 1. In the laboratory frame, the corresponding experimental signals — chiral doublet bands — are expected to be observed due to the quantum tunneling between systems with opposite chirality [1].

* Presented at the XXIV Nuclear Physics Workshop “Marie and Pierre Curie”, Kazimierz Dolny, Poland, September 20–24, 2017.

† Corresponding author: sqzhang@pku.edu.cn

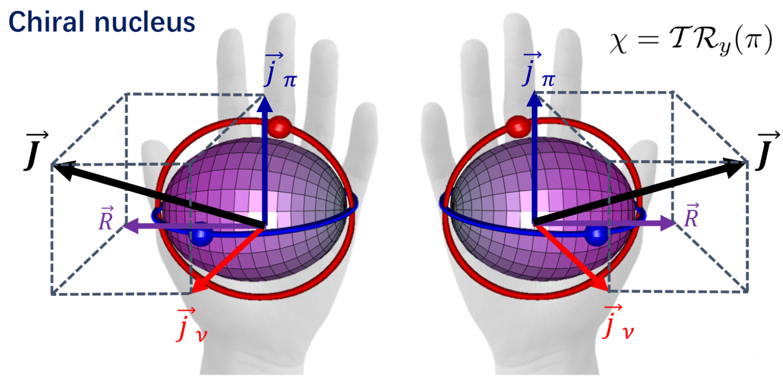

Fig. 1. A schematic picture of the left- and right-handed chiral systems for a triaxial nucleus. The collective, valence-proton, and valence-neutron angular momenta are denoted by $\vec{R}, \vec{j}_\pi$ and $\vec{j}_\nu$, respectively.

The chiral doublet bands were first observed in four $N = 75$ isotones in 2001 [6]. Up to now, candidate chiral doublet bands have been reported in around 40 nuclei in the $A \sim 80$ [7,8], 100 [9–13], 130 [6,14–23] and 190 [24–27] mass regions. Furthermore, a new phenomenon — multiple chiral doublet (MχD) — predicted by the microscopic covariant density functional theory in 2006 [28], was first observed in the nucleus ^{133}Ce [29], followed by more experimental evidences such as in ^{103}Rh [30] and ^{78}Br [8]. Lifetime measurements are essential to extract the absolute $B(\mathrm{M1})$ and $B(\mathrm{E2})$ transition probabilities, which are critical experimental observables in addition to the level energies. This has stimulated many experimental efforts aimed at identifying chiral doublet bands [31–37].

Many theoretical approaches have been developed and applied to investigate nuclear chirality, such as the particle rotor model (PRM) [1,38–46], the tilted axis cranking model (TAC) [1,47–50], the interacting boson fermion–fermion model (IBFFM) [51], and the projected shell model (PSM) [52]. In the mean-field level, the microscopic TAC approach can determine self-consistently the orientation of angular momentum vector and can be easily applied to the multi-particle configurations. However, the chiral symmetry is broken there and one has to go beyond the mean-field approximation to describe the energy splitting between the chiral doublet bands. The TAC plus random phase approximation (TAC+RPA) [33,53] provides the description of the regime of chiral vibration. More recently, the chiral geometry in the symmetry-restored states within the angular momentum projection method was revealed by using the *K plot* and *azimuthal plot* [54]. The collective Hamiltonian method provides another way out.

2. Collective Hamiltonian for chiral modes

Based on the tilted-axis-cranking solutions, one can construct collective Hamiltonian for chiral modes. Besides the region of chiral vibration naturally described by the collective Hamiltonian, the quantal tunneling in the region of chiral rotation can be described by considering the chiral fluctuations around mean-field minima. In one-dimensional collective Hamiltonian (1DCH) for chiral mode [55], the azimuth angle φ was introduced as chiral degree of freedom. The 1DCH has been applied to the system with symmetric particle–hole configuration $\pi h_{11/2} \otimes \nu h_{11/2}^{-1}$ coupled to a triaxial rotor with the triaxial deformation parameter $\gamma = -30°$. The 1DCH restored the broken chiral symmetry in TAC and reproduced well the exact solutions of energy spectra for chiral partners obtained by the PRM [55].

Later on, by considering both the azimuth angle φ and the polar angle θ as collective variables, a two-dimensional collective Hamiltonian (2DCH) was constructed [56]. In this work, the 2DCH was applied to the same system as in Ref. [55]. More excitation modes were obtained in the 2DCH than in the 1DCH, while the collective levels in the 1DCH have their correspondence in the 2DCH. The 2DCH remains invariant under the chiral and signature operators, and thus the broken chiral and signature symmetries in the TAC solutions are restored. By comparing the 2DCH results with the TAC ones and the exact solutions of PRM, it is shown that the 2DCH can reproduce well the PRM results in the high-spin region. However, in the low-spin region, the 2DCH provides decreasing energies with spin, which is inconsistent with the PRM results and the TAC ones. As demonstrated in Ref. [56], this problem can be avoided by including a constant vibrational frequency when calculating the mass parameters of collective Hamiltonian.

Furthermore, the collective Hamiltonian has also been developed to describe the wobbling motions in triaxial nuclei, including the simple, longitudinal, and transverse wobblers [57, 58]. In Ref. [59], it reproduced well the observed energy spectra of both the yrast and wobbling bands in ^{135}Pr.

3. Results with asymmetric particle–hole configuration

Here, we further apply the 2DCH to a system with asymmetric particle–hole configuration $\pi g_{9/2}^{-1} \otimes \nu h_{11/2}$ coupled to a triaxial rotor with $\gamma = -30°$. The coupling parameter $C_{\pi(\nu)}$ in the single-j shell Hamiltonian is chosen as $C_\pi = -0.2$ MeV for the proton hole and $C_\nu = 0.2$ MeV for the neutron particle. The moment of inertia of the triaxial rotor is taken as $\mathcal{J}_0 = 30\,\hbar^2/\text{MeV}$. This chiral system has been investigated by the triaxial PRM in Ref. [38].

The potential energy surfaces in the rotating frame, *i.e.*, the total Routhian $E'(\theta, \varphi)$ as a function of θ and φ, are shown in Fig. 2 at the frequencies $\hbar\omega = 0.10, 0.30, 0.50$ MeV. Since the D2 symmetry is held for a

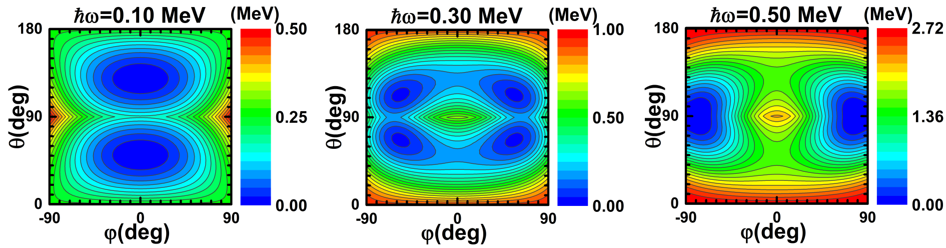

Fig. 2. Total Routhian surface calculations for one $g_{9/2}$ proton hole and one $h_{11/2}$ neutron particle coupled to a triaxial rotor with $\gamma = -30°$ at the frequencies $\hbar\omega = 0.10, 0.30, 0.50$ MeV. All energies are normalized with respect to the absolute minima. Note that different scales have been used in different panels.

quadrupole deformed nucleus, all the potential energy surfaces in Fig. 2 are symmetric with respect to the $\varphi = 0$ and $\theta = 90$ lines. At $\hbar\omega = 0.1$ MeV, the minima lie in the l–s plane ($\varphi = 0°$) with $\theta \sim 50°$ and $130°$, which correspond to the asymmetric particle–hole configuration used here. In Ref. [56], the minima for a symmetric particle–hole configuration lie in the l–s plane with $\theta = 45°$ and $135°$. With the increase of frequency, the minima change from $\varphi = 0°$ to $\varphi \neq 0°$, showing the transition to an aplanar rotation. At $\hbar\omega \sim 0.5$ MeV, the minima move close to $\theta = 90°$ and $\varphi = \pm 90°$, suggesting the transition of yrast mode to a principal axis rotation along the i-axis. It can also be seen that the energy surfaces are softer in the direction of φ at the low frequency, while softer in the direction of θ at the high frequency.

The mass parameters in 2DCH include $B_{\theta\theta}, B_{\theta\varphi}, B_{\varphi\theta}$, and $B_{\varphi\varphi}$, which are functions of (θ, φ) and are obtained by the cranking formula based on TAC solutions. As shown in Fig. 3, the $B_{\theta\theta}$ and $B_{\varphi\varphi}$ are symmetric with respect to $\varphi = 0°$ and $\theta = 90°$, whereas $B_{\theta\varphi}$ is antisymmetric. These behaviors, together with the symmetric collective potentials in Fig. 2, ensure the invariance of the collective Hamiltonian with the transformations of $\varphi \to -\varphi$ and $\theta \to 180° - \theta$.

The diagonalization of the 2DCH yields the energy levels and wave functions at each cranking frequency. In Fig. 4, the obtained collective energy levels at the frequencies $\hbar\omega = 0.10, 0.30$, and 0.50 MeV are shown (labeled "Total" in each panel). Since the 2DCH is invariant with the transformations $\theta \to 180° - \theta$ and $\varphi \to -\varphi$, one could group the eigenstates into four categories with different combinations of the symmetries P_θ and P_φ, *i.e.*, $(P_\theta P_\varphi) = (++), (+-), (-+)$, and $(--)$. The energy levels in different groups are associated with different phonon excitation modes. Energy levels in the group $(++)$ are from even-phonon excitations along both the θ and φ directions, whereas those in the group $(--)$ are from odd-phonon excitations in both directions. Similarly, energy levels in the group $(+-)$ $[(-+)]$

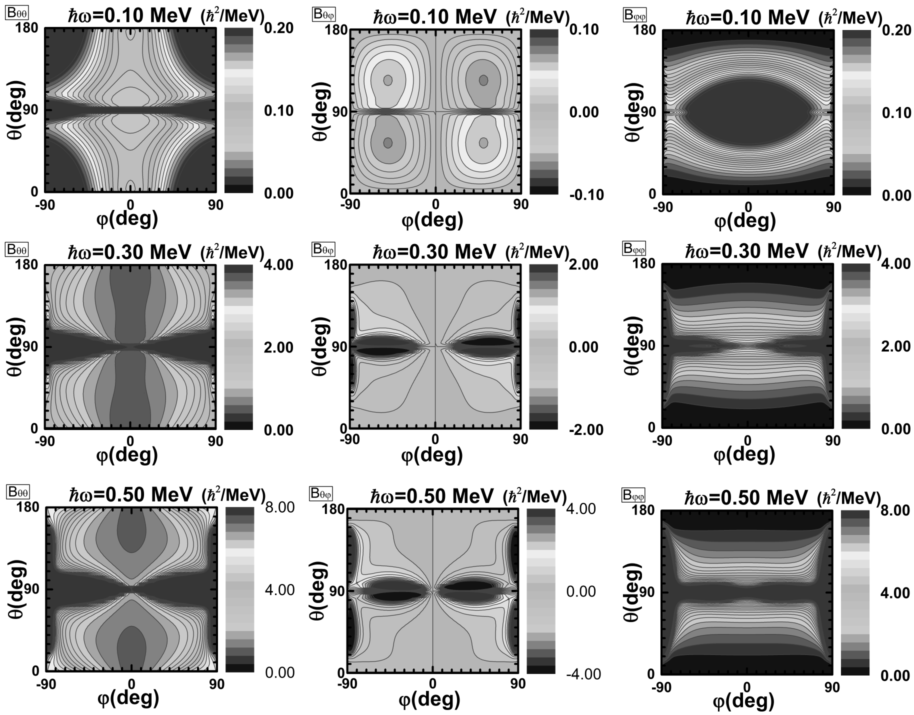

Fig. 3. The mass parameters $B_{\theta\theta}, B_{\theta\varphi}$, and $B_{\varphi\varphi}$ as functions of θ and φ at the frequencies $\hbar\omega = 0.10, 0.30$, and 0.50 MeV calculated based on TAC. The $B_{\varphi\theta}$ are identical to $B_{\theta\varphi}$. Note that different scales have been used in different panels.

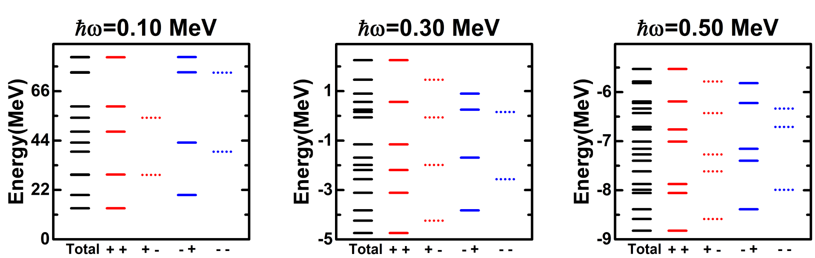

Fig. 4. Collective energy levels obtained from the two-dimension collective Hamiltonian at the frequencies $\hbar\omega = 0.10, 0.30, 0.50$ MeV. Note that different scales have been used in different panels.

correspond to even (odd) phonon excitations along the θ direction and odd (even) ones along the φ direction. The lowest energy level corresponds to the zero-phonon oscillation along both the θ and φ directions, and it is always in the group $(++)$.

In Fig. 4, the energy levels are sparsely distributed at low frequency $\hbar\omega = 0.10$ MeV, which is due to the neglecting of vibrational frequency when calculating mass parameters [56]. At $\hbar\omega = 0.10$ MeV, the lowest energy level in the group $(+-)$ is higher than that in the group $(-+)$, which is inversed at $\hbar\omega = 0.5$ MeV. This means that the collective motion along the θ direction is more favorable at low rotational frequencies, whereas the one along the φ direction is more favorable at high frequencies. This inversion can also be found in the 2DCH calculation for the symmetric particle–hole configuration [56].

In Fig. 5, the probability density distributions of the lowest states in the four groups (labeled E^1_{++}, E^1_{+-}, E^1_{-+}, E^1_{--}, respectively) are shown. These distributions are symmetric with respect to $\theta = 90°$ and $\varphi = 0°$ as expected, since the broken P_θ and P_φ symmetries in the TAC have been fully restored in the 2DCH. For $\hbar\omega = 0.10$ MeV, the peak of the density of E^1_{++} is located at $(\theta \approx 50°, \varphi = 0°)$, which corresponds to the minimum of the collective potential shown in Fig. 2. The density profiles of E^1_{+-} and E^1_{-+} are separated into two parts by $\varphi = 0°$ and $\theta = 90°$, respectively, reflecting the one-phonon excitation mainly along φ for E^1_{+-} and along θ for E^1_{-+}. The density profile of E^1_{--} is separated into four parts, which is consistent with the one-phonon excitations along both θ and φ. Furthermore, it can be

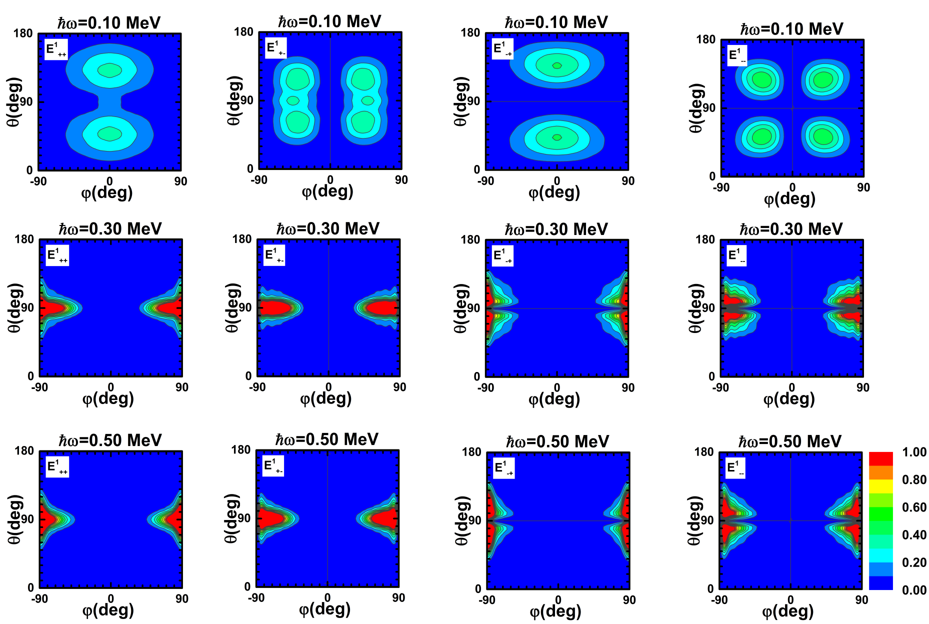

Fig. 5. The density profiles of the lowest states in groups $(++)$,$(+-)$,$(-+)$,$(--)$ at the frequencies $\hbar\omega = 0.10, 0.30$, and 0.50 MeV calculated by the 2DCH.

found that the phonon excitations along the φ and θ directions are weakly coupled. The above features also hold true for density profiles of other rotational frequencies.

4. Summary and perspective

In summary, the recent progress of collective Hamiltonian for the chiral modes is introduced. The collective Hamiltonian restores the broken chiral symmetry in the TAC solutions and could describe the chiral vibration and rotation on the same footing. Its validity was examined in Refs. [55, 56] by reproducing the exact PRM solutions. The results from applying the 2DCH to a nuclear system with an asymmetric particle–hole configuration $\pi g_{9/2}^{-1} \otimes \nu h_{11/2}$ coupled to a triaxial rotor are presented. The behaviors of the collective potentials and mass parameters, as well as the obtained collective levels and wave functions are similar to those for a symmetric chiral configuration [56].

Further implementation of the 2DCH on top of the selfconsistent tilted-axis-cranking covariant density functional theory [5,50,60–67] is interesting. The 2DCH can yield multiple chiral doublet bands [56] and, therefore, how to obtain properly the intraband and interband B(M1) and B(E2) values is an open question. To achieve a better description on chiral bands and the transitions, it is also interesting to construct the 2DCH based on the TAC calculation that constrained to the expectation value of total angular momentum $\langle J \rangle$. Works along the directions are in progress.

Stimulation discussions and fruitful collaborations with Q.B. Chen, R.V. Jolos, J. Meng, and P.W. Zhao are highly acknowledged. This work was partly supported by the Chinese Major State 973 Program No. 2013CB834400, the National Natural Science Foundation of China (grants No. 11375015, 11461141002, 11335002) and the Research Fund for the Doctoral Program of Higher Education (grant No. 20110001110087).

REFERENCES

[1] S. Frauendorf, J. Meng, *Nucl. Phys. A* **617**, 131 (1997).
[2] S. Frauendorf, *Rev. Mod. Phys.* **73**, 463 (2001).
[3] J. Meng, S.Q. Zhang, *J. Phys. G* **37**, 064025 (2010).
[4] A. Raduta, *Prog. Part. Nucl. Phys.* **90**, 241 (2016).
[5] J. Meng, P.W. Zhao, *Phys. Scr.* **91**, 053008 (2016).
[6] K. Starosta *et al.*, *Phys. Rev. Lett.* **86**, 971 (2001).

[7] S.Y. Wang *et al.*, *Phys. Lett. B* **703**, 40 (2011).
[8] C. Liu *et al.*, *Phys. Rev. Lett.* **116**, 112501 (2016).
[9] C. Vaman *et al.*, *Phys. Rev. Lett.* **92**, 032501 (2004).
[10] P. Joshi *et al.*, *Phys. Lett. B* **595**, 135 (2004).
[11] J. Timár *et al.*, *Phys. Lett. B* **598**, 178 (2004).
[12] P. Joshi *et al.*, *Eur. Phys. J. A* **24**, 23 (2005).
[13] Y.X. Luo *et al.*, *Phys. Lett. B* **670**, 307 (2009).
[14] T. Koike *et al.*, *Phys. Rev. C* **63**, 061304 (2001).
[15] A.A. Hecht *et al.*, *Phys. Rev. C* **63**, 051302 (2001).
[16] D.J. Hartley *et al.*, *Phys. Rev. C* **64**, 031304 (2001).
[17] R.A. Bark *et al.*, *Nucl. Phys. A* **691**, 577 (2001).
[18] X.F. Li *et al.*, *Chin. Phys. Lett.* **19**, 1779 (2002).
[19] T. Koike *et al.*, *Phys. Rev. C* **67**, 044319 (2003).
[20] G. Rainovski *et al.*, *Phys. Rev. C* **68**, 024318 (2003).
[21] A.J. Simons *et al.*, *J. Phys. G* **31**, 541 (2005).
[22] S.Y. Wang *et al.*, *Phys. Rev. C* **74**, 017302 (2006).
[23] S. Zhu *et al.*, *Phys. Rev. Lett.* **91**, 132501 (2003).
[24] D.L. Balabanski *et al.*, *Phys. Rev. C* **70**, 044305 (2004).
[25] E.A. Lawrie *et al.*, *Phys. Rev. C* **78**, 021305 (2008).
[26] P.L. Masiteng *et al.*, *Phys. Lett. B* **719**, 83 (2013).
[27] P.L. Masiteng *et al.*, *Eur. Phys. J. A* **50**, 119 (2014).
[28] J. Meng, J. Peng, S.Q. Zhang, S.-G. Zhou, *Phys. Rev. C* **73**, 037303 (2006).
[29] A.D. Ayangeakaa *et al.*, *Phys. Rev. Lett.* **110**, 172504 (2013).
[30] I. Kuti *et al.*, *Phys. Rev. Lett.* **113**, 032501 (2014).
[31] D. Tonev *et al.*, *Phys. Rev. Lett.* **96**, 052501 (2006).
[32] E. Grodner *et al.*, *Phys. Rev. Lett.* **97**, 172501 (2006).
[33] S. Mukhopadhyay *et al.*, *Phys. Rev. Lett.* **99**, 172501 (2007).
[34] E. Grodner *et al.*, *Phys. Lett. B* **703**, 46 (2011).
[35] E.O. Lieder *et al.*, *Phys. Rev. Lett.* **112**, 202502 (2014).
[36] N. Rather *et al.*, *Phys. Rev. Lett.* **112**, 202503 (2014).
[37] D. Tonev *et al.*, *Phys. Rev. Lett.* **112**, 052501 (2014).
[38] J. Peng, J. Meng, S.Q. Zhang, *Phys. Rev. C* **68**, 044324 (2003).
[39] T. Koike, K. Starosta, I. Hamamoto, *Phys. Rev. Lett.* **93**, 172502 (2004).
[40] S.Q. Zhang, B. Qi, S.Y. Wang, J. Meng, *Phys. Rev. C* **75**, 044307 (2007).
[41] B. Qi *et al.*, *Phys. Lett. B* **675**, 175 (2009).
[42] Q.B. Chen, J.M. Yao, S.Q. Zhang, B. Qi, *Phys. Rev. C* **82**, 067302 (2010).
[43] E. Lawrie, O. Shirinda, *Phys. Lett. B* **689**, 66 (2010).

[44] S.G. Rohoziński, L. Próchniak, K. Starosta, C. Droste, *Eur. Phys. J. A* **47**, 90 (2011).

[45] O. Shirinda, E.A. Lawrie, *Eur. Phys. J. A* **48**, 118 (2012).

[46] H. Zhang, Q.B. Chen, *Chin. Phys. C* **40**, 024102 (2016).

[47] V.I. Dimitrov, S. Frauendorf, F. Dönau, *Phys. Rev. Lett.* **84**, 5732 (2000).

[48] P. Olbratowski, J. Dobaczewski, J. Dudek, W. Płóciennik, *Phys. Rev. Lett.* **93**, 052501 (2004).

[49] P. Olbratowski, J. Dobaczewski, J. Dudek, *Phys. Rev. C* **73**, 054308 (2006).

[50] P.W. Zhao, *Phys. Lett. B* **773**, 1 (2017).

[51] S. Brant, D. Vretenar, A. Ventura, *Phys. Rev. C* **69**, 017304 (2004).

[52] G. Bhat *et al.*, *Phys. Lett. B* **738**, 218 (2014).

[53] D. Almehed, F. Dönau, S. Frauendorf, *Phys. Rev. C* **83**, 054308 (2011).

[54] F.Q. Chen *et al.*, *Phys. Rev. C* **96**, 051303(R) (2017).

[55] Q.B. Chen *et al.*, *Phys. Rev. C* **87**, 024314 (2013).

[56] Q.B. Chen *et al.*, *Phys. Rev. C* **94**, 044301 (2016).

[57] Q.B. Chen, S.Q. Zhang, P.W. Zhao, J. Meng, *Phys. Rev. C* **90**, 044306 (2014).

[58] Q.B. Chen, *Acta Phys. Pol. B Proc. Suppl.* **8**, 545 (2015).

[59] Q.B. Chen, S.Q. Zhang, J. Meng, *Phys. Rev. C* **94**, 054308 (2016).

[60] H. Madokoro, J. Meng, M. Matsuzaki, S. Yamaji, *Phys. Rev. C* **62**, 061301 (2000).

[61] J. Peng, J. Meng, P. Ring, S.Q. Zhang, *Phys. Rev. C* **78**, 024313 (2008).

[62] P.W. Zhao *et al.*, *Phys. Lett. B* **699**, 181 (2011).

[63] P.W. Zhao *et al.*, *Phys. Rev. Lett.* **107**, 122501 (2011).

[64] J. Meng, J. Peng, S.Q. Zhang, P.W. Zhao, *Front. Phys.* **8**, 55 (2013).

[65] P.W. Zhao, S.Q. Zhang, J. Meng, *Phys. Rev. C* **92**, 034319 (2015).

[66] P.W. Zhao, N. Itagaki, J. Meng, *Phys. Rev. Lett.* **115**, 022501 (2015).

[67] *Relativistic Density Functional for Nuclear Structure*, International Review of Nuclear Physics, (ed.) J. Meng, Vol. 10, World Scientific, Singapore 2016.